CrystEngComm

Accepted Manuscript

ROYAL SOCIETY OF CHEMISTRY

www.rsc.org/crystengcomm

Journal Name

ARTICLE

Fine-tuning halogen bonding properties of diiodine through halogen-halogen charge transfer – Extended [Ru(2,2'-bipyridine)$(CO)_2X_2$]·I_2 systems (X= Cl, Br, I)

Received 00th January 20xx,
Accepted 00th January 20xx

DOI: 10.1039/x0xx00000x

www.rsc.org/

Xin Ding[a], Matti J. Tuikka[a], Pipsa Hirva[*b], Vadim Yu. Kukushkin[c], Alexander S. Novikov[d], Matti Haukka[a*]

ABSTRACT: The current paper introduces use of carbonyl containing ruthenium complexes, [Ru(bpy)$(CO)_2X_2$] (X=Cl, Br, I), as halogen bond acceptors for I_2 halogen bond donor. In all structures the metal coordinated halogenido ligand is acting as the actual halogen bond acceptor. Diiodine, I_2, molecules are connected to the metal complexes through both ends of the molecule forming bridges between the complexes. Due to the charge transfer from Ru-X to I_2, formation of the first Ru-X···I_2 contact tends to generate negative charge on I_2 and redistribute the electron density anisotropically. If the initial Ru-X···I_A-I_B interaction causes a notable change in the electron density of I_2, the increased negative charge accumulates on the second iodine, I_B. The increased negative charge on I_B reduces its ability to act as halogen bond donor. With the [Ru(bpy)$(CO)_2Cl_2$] complex the electron density of I_2 molecule remains isotropic and it is acting as a symmetrical halogen bond donor for two metal complexes. With [Ru(bpy)$(CO)_2Br_2$] and [Ru(bpy)$(CO)_2I_2$] the Ru-X···I_A-I_B···X-Ru bridges are unsymmetrical with stronger and shorter Ru-X···I_A contact and weaker and longer Ru-X···I_B contact. In these cases the negative charge is accumulated on the more weakly bonded I_B atoms. QTAIM calculations were used to analyze the strength of the interactions and charge distribution in the metal complex and I_2 molecule in details. In accordance with the experimental data the QTAIM analyses show that the charge difference between the two ends of the I_2 molecule is increased in the order Ru-Cl···I_2 < Ru-Br···I_2 < Ru-I···I_2.

Introduction

Halogen bond (XB) has been a research topic of intensive interest over the last decade. XB has been exploited especially as a tool for crystal engineering, due to its almost linear directionality and relatively strong bond strength, which is comparable with hydrogen bonds. According to the IUPAC definition, halogen bond is denoted as R-X···Y system, in which R-X is the halogen bond donor and Y halogen bond acceptor. In principle, the halogen atom of the halogen bond donor can be attached to any R atom that can polarize and generate electrophilic region on the halogen. The halogen bond acceptor, in turn, is typically a molecular entity with a nucleophilic region.[1] The IUPAC definition states that "a halogen bond occurs when there is evidence of a net attractive interaction between an electrophilic region associated with a halogen atom in a molecular entity and a nucleophilic region in another, or the same, molecular entity".[1] The donor-acceptor interaction is mainly electrostatic in nature but other type of interactions such as charge transfer and dispersion forces may also play an important role in XB.

So far, organic compounds containing nitrogen, oxygen, or halogen atoms have been widely studied as electron donors i.e. the halogen bond acceptors.[2-9] Only a limited number of publications are concerning usage of metalorganic or organometallic XB acceptors [10-20]. This is the case even if metal complexes as acceptors could open up possibilities to utilize halogen bond as a tool for modifying their redox, magnetic, and optical properties as well as their chemical reactivity. [21-25] When a halogen atom is coordinated on an electron withdrawing organic moiety or a metal ion, the electron density around it is polarized. The electron density is concentrated perpendicular to the R-X or M-X bond and an electron poor area is formed as an extension to the R-X/M-X bond. However, unlike in organic R-X molecules, in M-X systems the polarization is usually not strong enough to generate positively charged σ-hole on the halogen atom (Fig. 1).

[a] University of Jyväskylä, Department of Chemistry, P.O. Box 35, FI-40014 University of Jyväskylä, Finland, e-mail: matti.o.haukka@jyu.fi
[b] University of Eastern Finland, Department of Chemistry P.O. Box 111, FI-80101, Joensuu, Finland.
[c] Department of Physical Organic Chemistry, St Petersburg State University, Stary Petergof 198504, Russian Federation.
[d] Institute of Chemistry, St. Petersburg State University, Stary Petergof 198504, Russian Federation.

† Electronic Supplementary Information (ESI) available: Crystallographic tables of structures **6**-**8**, Thermal ellipsoid plots of all crystal structures and bond critical points and bond paths for 1, 2, 4 and 5. See DOI: 10.1039/x0xx00000x. The detailed crystallographic data for structures **1**-**8** has been deposited with the Cambridge Crystallographic Data Centre as supplementary publication no. CCDC 1009208-1009215. Copies of this information may be obtained free of charge via www.ccdc.cam.ac.uk/data_request/cif.

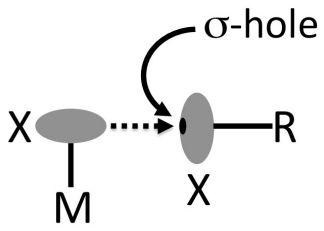

Figure 1. Distribution of electron density (the grey area) around the metal coordinated halogen atom and the halogen atom in R-X molecule. M-X is acting as XB acceptor and R-X as XB donor.

Despite the limited redistribution of electron density, the M-X unit can act as halogen bond acceptor i.e. electron donor with some directionality (Fig. 1). When the polarization of halogen on M-X is stronger, the M-X···X angle tends to be closer to 90°. Obviously, other factors such as intermolecular and intramolecular interactions may play a role as well and because of such factors the actual angle can deviate from the ideal value.

Just like organic R-X compounds, dihalogens, X_2, can serve as halogen bond donors. However, dihalogens comprise a special class of XB donors. Interactions between X_2 and an electron donor, D_e (XB acceptor), can often be rationalized in terms of charge transfer. According to this concept the electron donor donates electron density to the anti-bonding σ*-orbital of the X_2 molecule. As the result of electron donation, an attractive interaction is generated between the partially positively charged D_e^+ and partially negatively charged X_2^-. Strong charge transfer also leads to weakening of the X-X bond. Furthermore, the electron density within the X_2 molecule can also be unevenly distributed during the process. If the dihalogen molecule X_A-X_B is approaching the electron donor D_e with its X_A end, the negative charge tends to be accumulated on the non-interacting X_B halogen atom when forming the D_e···X_A-X_B system.[26,27] In the extreme case, the X_A-X_B bond is heterolytically broken and releasing, at least formally, negatively charged X_B^- ion and leaving positively charged X_A^+ coordinated on the electron donor. Although simple D_e-X^+ systems are usually rather unstable, several D_e-I^+-D_e systems, obtained via heterolytic cleavage of I_2, are known. The classic example is the cationic iodonium compound of $[I(py)_2]^+$.[28] Because of the unequal charge distribution on D_e coordinated X_2, the halogen bonded X_A and the dangling X_B ends are expected to behave differently. This does have an impact on reactivity of the I_2 molecule as well as the solid-state structures and packing of D_e···X_2 adducts. However, even if considerable number of XB systems involving X_2 molecules is known and a lot has been written about charge distribution in X_2 and polyhalides,[29] systematic attempts to exploit the redistribution of the charge on halogen bonded dihalogens has not been thoroughly studied.

In this paper we introduce a series of halogen-bonded systems using I_2 as a halogen bond donor and metal coordinated halogens of $[Ru(bpy)(CO)_2X_2]$ (bpy= 2,2'-bipyridine, X=Cl, Br, I) as weak halogen bond acceptors. The goal was to compare the ability of different ruthenium(II) bonded halogenido ligands to act as electron donors to I_2 through charge transfer and the effect it has on the charge distribution in I_2. All systems were characterized by single-crystal X-ray diffraction technique. A detailed analysis of the charge distribution was carried out by using computational QTAIM method.

Experimental

Materials

All reagents and solvents were obtained from commercial sources and were used as received without further purification. The XB acceptors $[Ru(bpy)(CO)_2X_2]$ (X=Cl, Br, I) were synthesized according to literature methods.[30, 31] The crystal structures of the pure $[Ru(bpy)(CO)_2X_2]$ (X=Cl, Br, I) metal complexes are known and reported in the literature. [30, 31] However, since only room temperature structures of these molecules have been reported the crystal structures of these complexes have been re-determined at 100K, and their details are not discussed in this paper.

Co-crystallization of I_2 and $[Ru(bpy)(CO)_2X_2]$ (X=Cl, Br, I)

The co-crystallizations were carried out in methanol or $CHCl_3$ solution. The metal complex and 2 equiv. of I_2 were dissolved separately at room temperature. The X-ray diffraction quality crystals were harvested after crystallization slow evaporation at R.T. or at 8°C.

$[Ru(bpy)(CO)_2Cl_2]\cdot I_2$ (1). The crystals were obtained by dissolving 5 mg of the metal complex and 7.9 mg of iodine into 5 ml of CH_3OH solvent. The crystallization was carried out at room temperature and crystals were harvested in 2 days.

$[Ru(bpy)(CO)_2Br_2]\cdot I_2$ (2). The crystals were obtained by dissolving 5 mg of the metal complex and 6.1 mg of iodine into 5 ml of $CHCl_3$ solvent. The crystallization was carried out at 8°C and the X-ray quality crystals were obtained in 4 weeks.

$[Ru(bpy)(CO)_2Br_2]\cdot I_2$ (3). The crystals were obtained by dissolving 5 mg of the metal complex and 6.1 mg of iodine into 5 ml of $CHCl_3$ solvent. The crystallization was carried out at 8°C and the crystals were harvested after 2 weeks.

$[Ru(bpy)(CO)_2I_2]\cdot I_2$ (4). The crystals were obtained by dissolving 5 mg of the metal complex and 4.9 mg of iodine into 5 ml of CH_3OH solvent. The crystallization was carried out at 8°C and the crystals were obtained in 4 weeks.

$[Ru(bpy)(CO)_2I_2]\cdot I_2$ (5). The crystals were obtained by dissolving 5 mg of the metal complex and 4.9 mg of iodine into 5 ml of CH_3OH solvent. The X-ray diffraction quality crystals were obtained in 2 weeks.

X-ray Structure Determinations.

The crystals of 1 - 8 were immersed in cryo-oil, mounted in a Nylon loop, and measured at a temperature of 100 K. The X-

ray diffraction data were collected on a Bruker Kappa Apex II Duo, Bruker Smart Apex II, or Bruker Kappa Apex II diffractometer using Mo Kα radiation (λ = 0.71073 Å). The APEX2[32] program package was used for cell refinements and data reductions. Structures were solved by direct methods or by charge flipping using the SHELXS-97[33] or SUPERFLIP[34] programs with the WinGX[35] graphical user interface. A multi-scan absorption correction based on equivalent reflections (SADABS)[36] was applied to all data. Structural refinements were carried out using SHELXL-97.[33] The hydrogen atoms were positioned geometrically and constrained to ride on their parent atoms, with C-H = 0.95 – 1.00 Å and U_{iso} = 1.2-1.5 U_{eq}(parent atom). The structure **7** was solved in a non-centrosymmetric space group Pn and refined as inversion twin with BASF refined to 0.093. The crystallographic details of structures **1** - **5** are summarized in Table 1. The crystallographic details of the previously reported structures of

Table 1. Crystal Data.

	1	**2**	**3**	**4**	**5**
empirical formula	$C_{12}H_8Cl_2IN_2O_2Ru$	$C_{13}H_9Br_2Cl_3I_2N_2O_2Ru$	$C_{13}H_9Br_2Cl_3I_2N_2O_2Ru$	$C_{12}H_8I_6N_2O_2Ru$	$C_{12}H_8I_4N_2O_2Ru$
fw	511.07	846.26	846.26	1074.67	820.87
temp (K)	100(2)	100(2)	100(2)	100(2)	100(2)
λ(Å)	0.71073	0.71073	0.71073	0.71073	0.71073
cryst. syst.	Triclinic	Monoclinic	Monoclinic	Orthorhombic	Triclinic
space group	$P\bar{1}$	$P2_1$	$P2_1/n$	$P2_12_12$	$P\bar{1}$
a (Å)	6.6617(2)	6.6553(1)	11.6841(6)	15.6811(6)	9.0961(16)
b (Å)	9.4643(2)	16.3426(4)	11.4179(6)	7.3656(3)	10.371(3)
c (Å)	13.0807(4)	10.2145(2)	17.2077(9)	9.4737(4)	10.572(3)
α (deg)	70.4400(10)	90	90	90	112.39(3)
β (deg)	80.9530(10)	97.865(1)	105.946(1)	90	93.49(3)
γ (deg)	83.3070(10)	90	90	90	90.70(2)
V (Å^3)	765.64(4)	1100.53(4)	2207.3(2)	1094.22(8)	919.8(4)
Z	2	2	4	2	2
ρ_{calc} (Mg/m^3)	2.217	2.554	2.547	3.262	2.964
μ(Mo Kα) (mm^{-1})	3.389	7.522	7.501	9.188	7.568
No. reflns.	28379	26564	66442	22615	8005
Unique reflns.	8276	7286	6749	5875	4225
GOOF (F^2)	1.018	0.994	1.052	1.088	1.051
R_{int}	0.0253	0.0333	0.0360	0.0327	0.0222
R1[a] ($I \geq 2\sigma$)	0.0211	0.0239	0.0204	0.0193	0.0338
wR2[b] ($I \geq 2\sigma$)	0.0440	0.0542	0.0454	0.0400	0.0879

[a] $R1 = \Sigma||F_o| - |F_c||/\Sigma|F_o|$. [b] $wR2 = [\Sigma[w(F_o^2 - F_c^2)^2]/\Sigma[w(F_o^2)^2]]^{1/2}$.

Table 2. Selected bond angles and length of co-crystals **1-5**. The distances are in angstroms [Å] and the angles in degrees [°]

#	X1···I3	X2···I4	I3-I4	I4-I3···X1	I3-I4···X2
1	3.0421(3)	3.0421(3)	2.7317(2)	174.566(8)	174.566(8)
2	3.2938(4)	3.3627(3)	2.7212(3)	170.28(1)	173.80(1)
3	3.2381(3)	3.3001(3)	2.7215(3)	175.405(9)	174.164(9)
4	3.1984(2)	3.7984(3)	2.7554(2)	177.941(7)	152.083(6)
5	3.2553(13)	3.4108(15)	2.7572(12)	172.75(2)	166.50(2)

6 – **8**[30, 31], are given only as supplementary material (Figures S6-S8). Molecular graphics were performed with the UCSF Chimera package.[37]

Computational methods

The wavefunctions of the models in experimental geometries were computed by Gaussian 09 program package[38] at the DFT level of theory. PBE0 hybrid functional[39] with LANL2TZ(f)[40-42] basis set for Ru, LANL2DZspdf[43] basis set for I, LANL2DZdp[40-42] basis set for Cl and Br, and a standard basis set 6-311++G(d,p) for C, O, N and H atoms were used in the calculations. Topological charge density analysis according to the Quantum Theory of Atoms in Molecules (QTAIM)[44] of the computational wavefunctions was performed with the AIMAll program[45]. The models used for the computational analysis are shown in the supporting information.

Results and Discussion

Chlorido ligand as a halogen bond acceptor.

In general, chlorine is usually not seen as a particularly good halogen bond acceptor or donor compared to its heavier analogs. This is simply because chlorine is relatively small and not as easily polarizable as the heavier halogens. However, as a metal coordinated ligand it is capable of acting as an electron donor i.e. XB acceptor for a suitable XB donor such as I_2. Co-crystallization of the $[Ru(bpy)(CO)_2Cl_2]$ with I_2 led to a dimeric structure where the complexes were linked through symmetrical halogen bonds between the Cl ligands and the bridging I_2 molecule (Fig. 2). However, only one of the Cl

ligands of the complex was involved in halogen bonding. The distance between Cl and I was found to be 3.0421(3) Å, which is about 82% of the sum of van der Waals radii of Cl and I. A series of weak Cl···H and I···H hydrogen bonds together with π-π interactions support the overall molecular assembly linking the dimeric units into a 3D network (Fig. 3).

Since in **1** both ends of I_2 are involved in identical halogen bonds, the charge densities on both ends of I_2 are also expected to be identical i.e. both ends are able to act as halogen bond donors in exactly the same way. Because of the symmetrical bridge, the impact of the charge transfer is also expected to be relatively weak. Strong charge transfer from chloride ligand to one end of the I_2 molecule should weaken the XB contact of the second I atom. Furthermore, if there were a strong charge transfer from both chloride ligands, the I-I bond should be considerably weakened, yet the I-I distance in **1** (2.7317(2) Å) is relatively close to the typical I-I distance in a non-halogen bonded I_2 molecule (2.720(8)Å) in solid state.[46]

The I-I···Cl angle in **1** is 174.566(8)°, which is close to the optimum value of 180° for a typical XB bond. In the ideal case the Ru-Cl···I angle is should be close to 90° due to the polarization of the electron density around the chlorido ligand. In structure **1** this angle is 115.76(1)° indicating that the electron density around the Cl is indeed polarized but not strongly enough to force the I_2 molecule in the ideal angle. Obviously, since the XB contact is not particularly strong, the packing effects influence also the Ru-Cl···I angle.

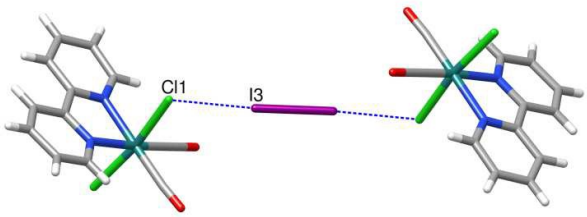

Figure 2. Halogen bonding interactions between the Cl1 and I3 atoms in the co-crystal **1**. Grey atoms represents C; white H; blue N; dark green Ru, red O; light green Cl and violet I.

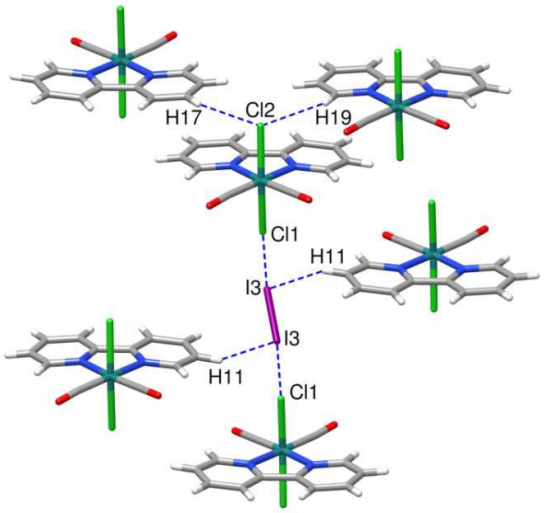

Figure 3. The 3D network of **1**. Hydrogen bonding interactions in the co-crystal **1**. The color scheme is the same as in Figure 1.

Bromido ligand as a halogen bond acceptor.

The electron density in the bromido ligand is more diffuse than in Cl and therefore it tends to be more polarizable by the metal cation than Cl. By using similar co-crystallization conditions as with the chlorido analog we were able to obtain two variants of $[Ru(bpy)(CO)_2Br_2]\cdots I_2$ co-crystals (**2** and **3** shown in Figs. 4-6). Again, the I_2 molecule was connected through both its I atoms linking two $[Ru(bpy)(CO)_2Br_2]$ complexes together by Br···I-I···Br halogen bonds (Figure 4). Unlike in **1**, both halogenido ligands of the $[Ru(bpy)(CO)_2Br_2]$ molecule, were now involved in halogen bonding. Furthermore, the two XB bonds were not identical. In **2**, the shorter Br···I distance was 3.2938(4) Å and the longer one 3.3627(3) Å corresponding to 86% and 88% of the sum of Van der Waals radii of Br and I, respectively. In **3** the Br···I distances were 3.2381(3)Å (85 %) and 3.3001(3)Å (86%). The main difference between the structures **2** and **3** was the overall packing of the complexes. The structure **2** was crystallized in the chiral space group $P2_1$ and it consists of parallel chains of complexes linked together with I_2 molecules (Fig. 5). Structure **3** was crystallized in the centrosymmetric space group $P2_1/n$ and the complexes formed structures where the molecules of the neighboring chains were facing opposite directions (Fig. 6). In both cases the adjacent chains were held together by additional C-H···Br hydrogen bonds. Both **2** and **3** also contained chloroform of crystallization that was weakly hydrogen bonded to one of the bromido ligands.

Since the XBs involving I3 and I4 ends of the I_2 molecule (Figs. 4-6) are different in both co-crystals **2** and **3**, it is expected that the charge transfer on the shorter Br1···I3 contact is slightly increased compared to the other end of I_2. If this is the case the electron density in I_2 is also expected to be changed and the electron density should be increased on I4 end of the diiodine. Such distribution of charges in diiodine molecule would mean that the I4 end is less prone to act as XB donor

because of the increased electron density and reduced σ-hole on it. However, even though the charge transfer was expected to be enhanced in **2** and **3** compared to the structure **1**, the elongation of the I-I bond remained moderate. The I-I distances were 2.7212(3)Å and 2.7215Å(3) in structures **2** and **3** respectively. In fact, they are even slightly shorter than in the case of **1**. Even if the XBs involving the different ends of I_2 molecule are not identical, the geometric differences are subtle. First of all, in **2** the I-I···Br angles are 170.28(1)° for the shorter and 173.80(1)° for the longer XB contact. Similarly, the Ru-Br···I angles are 101.30(1)° and 102.27(1)° for the shorter and longer halogen bonds. In structure **3** the corresponding values are I-I···Br: 175.405(9), 174.164(9) and Ru-Br···I: 101.66(1), and 102.57(1). The more polarized electron density around the bromide ligand favors Ru-Br···I angles that are closer to the 90° compared to the Ru-Cl···I values in **1**.

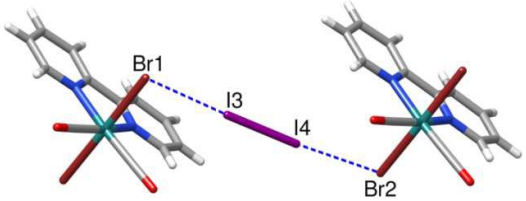

Figure 4. Halogen bonding interactions between Br1···I1-I2···Br2 in the co-crystal **2**. Dark red represents Br atoms. Otherwise the color scheme is the same as in Figure 2.

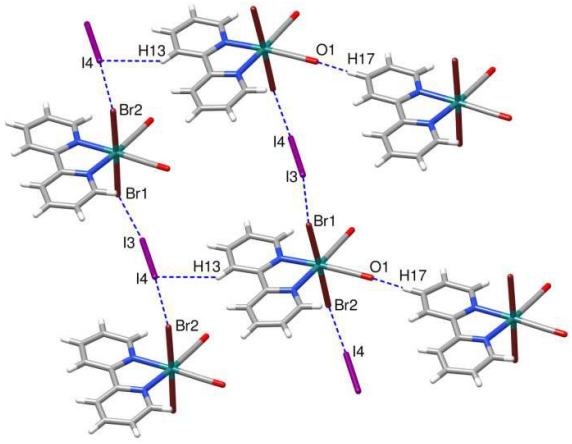

Figure 5. Orientation of the molecular units in the co-crystal **2**. The color scheme is the same as in Figure 4.

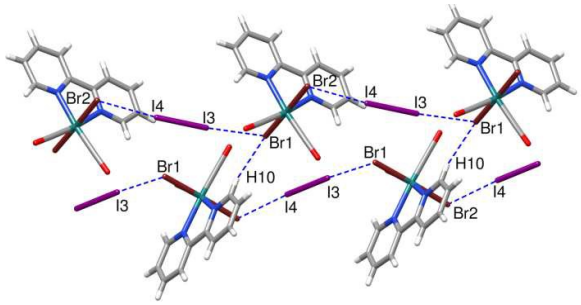

Figure 6. Halogen bonding and hydrogen bonding interactions in the co-crystal **3**. The color scheme is the same as in Figure 4.

Iodido ligand as a halogen bond acceptor.

Iodine is probably the most popular halogen bond donor, but due to its strong polarization ability, it is also capable of acting as effective XB acceptor. When $[Ru(bpy)(CO)_2I_2]$ complexes were co-crystallized with I_2 two types of structures (**4** and **5**) were again obtained. Just like with $[Ru(bpy)(CO)_2Br_2]$, both halogenido ligands of the $[Ru(bpy)(CO)_2I_2]$ complexes were participating in halogen-halogen interactions with I_2. In structure **4** the two ends of the I_2 halogen bond donor interact with the metal coordinated iodido ligand quite differently (Fig. 7). The shorter Ru-I···I3 distance was only 3.1984(2) Å (81%) while the longer, Ru-I···I4 was 3.7984(3) Å (96%). This indicates that the charge transfer is enchanced compared to adducts **1**-**3**. Because of the stronger charge transfer in the case of adduct **4**, the I-I bond of the I_2 molecule was elongated by about 0.03 Å (2.7554(2)). If the shorter Ru-I···I3 contact is the dominating contact from the charge transfer point of view, it is expected that the negative charge on I_2 is accumulated on I4. This, in turn, would mean that it is less eager to act as XB donor weakening the second XB contact. Such an assumption is supported by the geometry of the Ru-I···I3-I4···Ru system. In the stronger contact the I4-I3···I angle is nearly linear 177.941(7)°, while in the weaker contact I3-I4···I it is only 152.083(6)°. The latter is already quite far from the typical I-I···acceptor angle of 180°. Also, the Ru-I···I3 angle of 97.91(1) is close to the optimal angle of 90°, while the Ru-I···I4 is clearly wider (104.26(1)°). Based on the geometry, the donor – electron acceptor nature of the participating iodine atoms in Ru-I···I4 contact is no longer obvious. It could be even said that this type of contact is no longer a true halogen bond, although there are reports where similar contacts have been defined as amphoteric XB.[47] Even if the I_2 bridge is uneven in **4** it can still be seen as a bridge that organizes the metal complexes to infinite chains. The neighboring chains are connected via hydrogen bonds between H11 and I4 (Fig. 8). It is worth mentioning that only the less strongly halogen bonded I4 participates in hydrogen bonding. This is also in agreement with the assumption of increased negative charge on I4. The extra electron density favors contacts with electron acceptors i.e. hydrogen bond donor in this case.

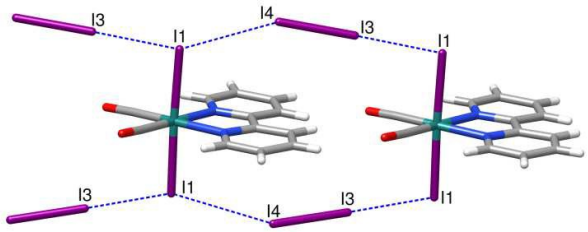

Figure 7. Chain structure formed by halogen bonding and hydrogen bonding in the co-crystal **4**. The color scheme is the same as in Figure 1.

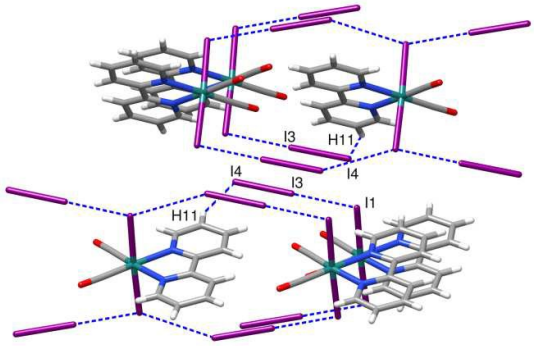

Figure 8. Hydrogen bonding interactions between I_4 and H11 atoms in the co-crystal **4**. The color scheme is the same as in Figure 1.

The structure **5** is completely different from the structure **4**. First of all, in terms of Ru-I···I distances the two XBs are much closer to each other than in **4**. This could be taken as a sign of weaker charge transfer from the complex to the diiodine molecule. The Ru-I···I distances were 3.2553(13)Å (82%) and 3.4108(15)Å (86%) and the angles I-I···I 172.75(2)° and 166.50(2)°, respectively. Similarly, the Ru-I···I angles are quite close i.e. 97.81(2)° and 98.90(2)°. But even if the differences in **5** are less clear than in **4**, the same trends in the geometry can be seen. Unlike any of the systems **1**-**4** the complexes in **5** do not form I_2 linked chains. Instead, both halogen bonds are used to connect two complexes into a dimeric structure (Fig. 9). These dimeric units are then linked together through weak C-H···I hydrogen bonds (Fig. 10).

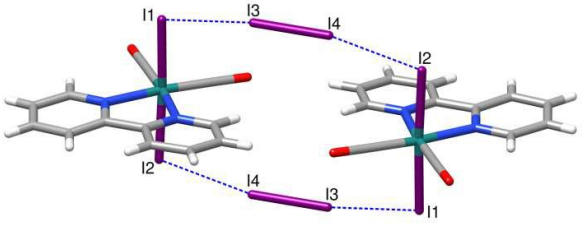

Figure 9. Dimeric structure of the co-crystal **5** formed through halogen bonded I_2 bridges. The color scheme is the same as in Figure 1.

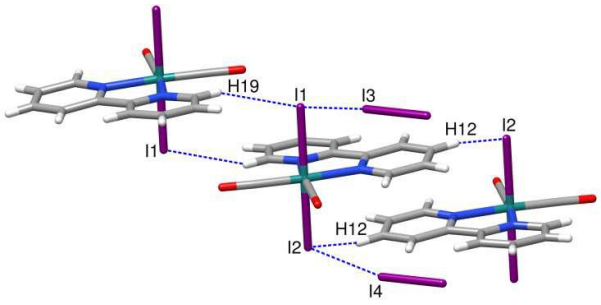

Figure 10. Hydrogen bonding interactions in structure **5**. The color scheme is the same as in Figure 1.

Computational results.

To gain more detailed information about the halogen bonding we performed QTAIM analysis using the wavefunctions originating from the experimental structures. The summary of the charge density analysis for structures **1**-**5** is presented in table **3**.

Table 3. Selected properties of the electron density according to the QTAIM analysis of the halogen bonding in structures **1**-**5**. In the case of structures 2-5 both the stronger and the weaker contacts were analysed. Parameters are: d = I···X distance [Å]; $\rho(r_c)$ = electron density at the bond critical point [eÅ^{-3}]; Lapl. =Laplacian of the electron density [eÅ^{-5}]; $G(r_c)$ = kinetic energy density [kJmol^{-1}]; $V(r_c)$ = potential energy density [kJmol^{-1}]; $H(r_c)$ = total energy density [kJmol^{-1}]; $E_{int} = V(r_c)/2$ [kJmol^{-1}].

#	d	$\rho(r_c)$	Lapl.	$G(r_c)$	$V(r_c)$	$H(r_c)$	$\lvert V\rvert/G$	E_{int}
1	3.042	0.168	1.939	39.3	-36.7	2.49	0.94	-18.4
2	3.294	0.132	1.301	26.6	-23.9	2.76	0.90	-12.0
2	3.363	0.116	1.137	23.3	-20.2	3.03	0.87	-10.1
3	3.238	0.145	1.452	29.7	-27.3	2.39	0.92	-13.7
3	3.300	0.129	1.291	26.4	-23.6	2.85	0.89	-11.8
4	3.198	0.202	1.896	36.1	-39.3	-3.20	1.09	-19.7
4	3.798	0.069	0.609	12.6	-10.0	2.65	0.79	-5.0
5	3.255	0.184	1.699	32.8	-34.4	-1.58	1.05	-17.2
5	3.411	0.137	1.292	25.6	-24.0	1.61	0.94	-12.0

In all cases the computational model system contained two metal complexes and, depending on the structure, one to six I_2 molecules. Because of the high symmetry, only one I_2 molecule was used for structure **1**, and the model corresponds to structure in Figure 2. For structure **2** a model like in Figure 5 was used, but with only one halogen bonded chain. The same applies for the structure **3**. For structure **4**, the model was like the structure in Figure 7, but with six I_2 molecules to maintain the bifurcated nature of the iodide ligands. For structure **5** the model was similar to the one shown in Figure 9. The models are described in details in the supplementary material (Figures S9-S13).

Analysis of the critical points

The QTAIM analyses revealed bond critical points (BCP) between the halogenido ligands and I_2 in all of the structures. The BCPs were found for all of the halogen bonds displayed in Figures 2, 4, 7 and 9. In addition, some BCPs were found between the I_2 molecules and bipyridine hydrogen and carbon atoms. BCPs were also found between the carbonyl groups

and bipyridine hydrogens. The bond critical points and bond paths are summarized in the Figures S9-S13 in the supplementary data.

The electron densities and laplacian values on these BCPs were comparable with the typical values reported for XBs involving metal complexes.[21, 48] According to a review by Carlo Gatti, classification of the nature of the bonding interactions can be done by looking at certain properties of the charge density at the bond critical points.[49] The halogen bonding interactions in **1**-**3** clearly show typical properties of closed shell interactions (Table 3), since they exhibit relatively small electron density, positive Laplacian of electron density and positive total energy density $H(r_c)$. Also the ratio between the potential energy density $V(r_c)$ and the kinetic energy density $G(r_c)$ can be used to characterize the nature of the interactions: $|V(r_c)|/G(r_c)$ values less than 1 indicate electrostatic interactions and values larger than 2 suggest covalent interactions.[49] In crystals **1**-**3** this value is clearly less than 1, again showing the closed shell halogen bonding interactions. However, for the strongest I1···I3 halogen bonds in **4** and **5**, the Laplacian is still positive, but $H(r_c)<0$, and $1<|V(r_c)|/G(r_c)<2$, which would put them inside the transit region between closed shell and covalent interactions. Based on the computational results it seems that the nature of the interactions changes from purely electrostatic non-covalent interaction in $[Ru(bpy)(CO)_2X_2]$, where X = Br or Cl, towards slightly more covalent interaction in $[Ru(bpy)(CO)_2I_2]$. The results also support nicely the idea that the charge transfer is strongest in structures **4** and **5**.

Cheng et al. have studied strength of halogen bonds between group 10 metal monohalides and C_6F_5I halogen bond donor. According to their results, the order of the interaction energies follow order Br < Cl < F.[50] The systems with fluorido ligand corresponds to the strongest and systems with bromido to the weakest halogen bonds. Johnsson et al. have reported similar order by comparing halogen bonded platinum complexes with Cl and Br ligands.[51] Espinosa et al. have suggested that the interaction energies (E_{int}) can be estimated by analysing the local potential energy density at the BCP: $E_{int} = V(r_c)/2$.[52] Even though this relation was originally developed for hydrogen bonding interactions, It has been shown that linear correlation between interaction energy and potential energy density can be found for other non-covalent interactions as well. This approach has been successfully applied even for metallophilic contacts.[53] When comparing the E_{int} values of **1**, **3**, and **4** for the strongest XBs, the order is I > Cl > Br, which are in line with the previous reports.[50, 51] However, the differences are relatively small and depend on the detailed structure of the adduct. From purely electrostatic point of view, the expected order of E_{int} would be Cl > Br > I. In the case of **4** and **5**, the slight increase in covalency is probably the reason behind the increased E_{int} value and strengthening of the halogen bond.

Charge transfer and distribution of charges on I_2

The distributions of charges have been studied in several halogen-bonded systems containing iodine. However, in most cases the focus has been on overall charges of the iodine moieties. Less attention has been paid on the internal charge distribution on the halogen bonded I_2. To put the properties of the electron densities found in M-X···I_2 systems into perspective, we carried out a QTAIM analysis of the strong halogen bonding adduct of pyridine···I_2. In this structure, only one end of the I_2 is involved in halogen bonding. The second iodine is dangling and does not form XBs. The details of the QTAIM results are given as supplementary material. According to the experimental Py···I_2 structure,[54] the N···I halogen bond distance is short, 2.425(8) Å, which is about 69% of the sum of vdW radii of N and I. Accordingly, the QTAIM analysis showed considerable electron sharing at the I···N bond critical point ($|V_b|/G_b$ was 1.33) and hence larger total energy density of -31.9 $kJmol^{-1}$ and E_{int} value of -64.3 kJ/mol. The strong contact indicates also strong charge transfer from the pyridine to I_2. The impact of charge transfer from the XB acceptor to I_2 is expected to be two-fold. Firstly, it increases the negative charge of the I_2 molecule and secondly it changes the internal charge distribution within I_2. The total charge of I_2 in Py···I_2 is -0.185, which is not particularly high. However, this is because of the uneven charge distribution. The charge of the halogen-bonded iodine is already positive, +0.076, while the charge of the second, non-halogen bonded iodine is -0.261. Such a clear distribution of charges is typical for halogen bonds with strong charge transfer. Similar redistribution of charges have also been observed on strongly halogen bonded Br_2.[26] The change in the internal charge distribution often seems to be even more indicative parameter for charge transfer than the I-I distance or total charge of the I_2 molecule. The elongation is clear in cases where the charge transfer is strong, for example, in Py···I_2 where the I-I distance is elongated to 2.8043(9) Å[54]

Compared to the Py···I_2 adduct, the impact of XBs on charge distributions on I_2 molecule in structures **1**-**5** are less pronounced because of the weaker halogen bonds (Table 4). In cases **2**-**5** with uneven charge distribution on I_2 molecule, the weaker halogen bond always involves the more negatively charged iodine (I4). This indicates that the polarization of the internal charge distribution does have an impact on the halogen bond donor properties of the iodine atoms in I_2 molecule. In structure **1**, the I_2 is acting as a symmetrical bridge between the metal complexes. The total charge of I_2 is -0.136 and both ends of the iodine molecule possess identical charges. The total charge of I_2 in structure **2**, is practically identical with the structure **1**. However, the negative charge is concentrated on the iodine atom I4 that is involved in the weaker XB (Fig. 4). In the structure **3**, the total charge of the I_2 molecule is somewhat higher but the charge distribution resembles closely the distribution found in structure **2**. The highest total charges of I_2 can be found in $[Ru(bpy)(CO)_2I_2]\cdots I_2$ co-crystals **4** and **5**. Interestingly, the highest negative charge of I_2 is not in the adduct **4**, in which the bridging I_2 is involved in the strongest and the weakest XBs. However, in this structure the uneven distribution of the negative charge is most pronounced reducing the capability of the more negatively charged iodine to act as halogen bond donor.

Table 4. QTAIM charges of halogen bonded I_2 molecules for structures 1-5.

Co-crystal	Tot. Charge of I_2	[a]Charge1	[b]Charge2	C1/C2
1	**-0.136**	-0.068	-0.068	1
2	**-0.137**	-0.064	-0.073	0.88
3	**-0.156**	-0.073	-0.083	0.88
4	**-0.168**	-0.057	-0.111	0.51
5	**-0.234**	-0.097	-0.137	0.71

[a]Charge 1 refers to the charge on the I3 atom with the shorter halogen bond distance.
[b]Charge 2 refers to the charge on the I4 atom with the longer halogen bond distance.
C1/C2 is the ratio of charges I3/I4

Conclusions

The XB bonds between I_2 and five ruthenium(II) complexes $[Ru(bpy)(CO)_2X_2]$ (X = Cl, Br, I) were analyzed by using single-crystal X-ray structures and computational QTAIM technique. The structures consist of metal complexes and bridging I_2 molecules that interact with the complexes through halogen-halogen interactions. In all studied systems the metal coordinated halogen ligands act as a halogen bond acceptors and both iodines of the bridging I_2 molecule as halogen bond donors. Both experimental structures and QTAIM analyses of the properties of bond critical points show that the halogen bond strength decreases in the order Ru-I···I_2› Ru-Cl···I_2› Ru-Br···I_2 when the strongest XB contacts are compared. In all structures the halogen bonding generates negative overall charge on the I_2 molecule due to the charge transfer from the complex to the diiodine. In the case of $[Ru(bpy)(CO)_2Cl_2]$···I_2 adduct, the iodine bridge is symmetrical with identical M-Cl···I-I···Cl-M distances. In this system, the negative charge is evenly distributed on the I_2 molecule. When the metal complex contains more polarizable halogenido ligands as the halogen bond acceptors i.e. Br and especially I, the I_2 bridge tends to become asymmetrical with different M-X···I-I···X-M distances. In such a case also the internal charge distribution of I_2 becomes uneven. The negative charge accumulates on the iodine, which is involved in the weaker halogen bond. The results indicate that if one end of the I_2 molecule is involved in a relatively strong halogen bond with a noticeable charge transfer contribution, the accumulation of the negative charge on the second iodine is reducing its capability to act as halogen bond donor weakening the second XB. Because of this, the halogen bonding properties of the two iodines in I_2 molecule are changed. The increased electron density on the second iodine makes it more prone to act as electron donor and therefore it forms more easily for example hydrogen bonds. The formation of a strong halogen bond accompanied with redistribution of the charge can thus be used to change the coordinative behaviour of diiodine, which in turn, can be exploited for example in designing and building supramolecular assemblies.

ACKNOWLEDGMENT

Financial support provided by the Academy of Finland (project 139571 M. H., M.T., X.D) and the Inorganic Materials Chemistry Graduate Program (EMTKO) as well as COST Action 1302 are gratefully acknowledged. The computational work has been facilitated by access to the Finnish Grid Infrastructure resources.

Notes and references

1 G. R. Desiraju, P. S. Ho, L. Kloo, A. C. Legon, R. Marquardt, P. Metrangolo, P. Politzer, G. Resnati and K. Rissanen, *Pure Appl. Chem.,* 2013, **85**, 1711-1713 (DOI:10.1351/PAC-REC-12-05-10).
2 P. Metrangolo, H. Neukirch, T. Pilati and G. Resnati, *Acc. Chem. Res.,* 2005, **38**, 386-395 (DOI:10.1021/ar0400995).
3 A. C. Legon, *Phys. Chem. Chem. Phys.,* 2010, **12**, 7736-7747 (DOI:10.1039/c002129f [doi]).
4 P. Politzer, P. Lane, M. C. Concha, Y. Ma and J. S. Murray, *J. Mol. Model.* 2006, **13**, 305-311 (DOI:10.1007/s00894-006-0154-7).
5 L. C. Roper, C. Präsang, V. N. Kozhevnikov, A. C. Whitwood, P. B. Karadakov and D. W. Bruce, *Cryst. Growth Des.,* 2010, **10**, 3710-3720 (DOI:10.1021/cg100549u).
6 M. G. Sarwar, B. Dragisic, S. Sagoo and M. S. Taylor, *Angewandte Chem. Int. Ed.* 2010, **49**, 1674- 1677 (DOI:10.1002/anie.200906488).
7 S. Tsuzuki, A. Wakisaka, T. Ono and T. Sonoda, *Chem. Eur. J.* 2012, **18**, 951-960 (DOI:10.1002/chem.201102562).
8 K. J. P. Davy, J. McMurtrie, L. Rintoul, P. V. Bernhardt and A. S. Micallef, *CrystEngComm,* 2011, **13**, 5062-5070 (DOI:10.1039/c1ce05344b).
9 P. Metrangolo, G. Resnati, T. Pilati, R. Liantonio and F. Meyer, *J. Polymer Sci. Part A: Polymer Chem.* 2007, **45**, 1-15 (DOI:10.1002/pola.21725).
10 P. Smart, Á Bejarano-Villafuerte and L. Brammer, *CrystEngComm,* 2013, **15**, 3151-3159 (DOI:10.1039/c3ce26890j).
11 J. E. Ormond-Prout, P. Smart and L. Brammer, *Cryst. Growth Des.* 2012, **12**, 205-216 (DOI:10.1021/cg200942u).
12 H. M. Titi, R. Patra and I. Goldberg, *Chem. Eur. J.* 2013, **19**, 14941-14949 (DOI:10.1002/chem.201301857).
13 J. Le Bras, A. H. and V. J., *Inorg. Chem.,* 1998, **37**, 5056 (DOI:10.1021/ic971427i).
14 K. F. Tebbe, A. Grafe-Kavoosian and B. Freckmann, *Z. Naturforsch. , B: Chem. Sci.,* 1996, **51**, 999-1006.
15 C. Wieczorrek, *Acta Crystallogr. C.* 2000, **56**, 1085-1087 (DOI:10.1107/S0108270100008830).
16 N. Masuhara, S. Nakashima and K. Yamada, *Chem. Lett.,* 2005, **34**, 1352-1353 (DOI:10.1246/cl.2005.1352).
17 R. A. Gossage, A. D. Ryabov, A. L. Spek, D. J. Stufkens, J. A. M. van Beek, R. van Eldik and G. van Koten, *J. Am. Chem. Soc.,* 1999, **121**, 2488-2497.
18 S. Blanchard, F. Neese, E. Bothe, E. Bill, T. Weyhermüller and K. Wieghardt, *Inorg. Chem.,* 2005, **44**, 3636-3656 (DOI:10.1021/ic040117e).
19 S. Zhao, R. Wang and S. Wang, *Organometallics,* 2009, **28**, 2572-2582 (DOI:10.1021/om900022n).
20 L. Brammer, G. Mínguez Espallargas and S. Libri, *CrystEngComm,* 2008, **10**, 1712-1727 (DOI:10.1039/b812927d).

21 M. Tuikka, M. Niskanen, P. Hirva, K. Rissanen, A. Valkonen and M. Haukka, *Chem. Commun.* 2011, **47**, 3427-3429 (DOI:10.1039/c0cc05726f [doi]).
22 M. Tuikka, P. Hirva, K. Rissanen, J. Korppi-Tommola and M. Haukka, *Chem. Commun.,* 2011, **47**, 4499-4501 (DOI:10.1039/c1cc10491h [doi]).
23 E. Coronado and P. Day, *Chem. Rev.,* 2004, **104**, 5419-5448 (DOI:10.1021/cr030641n).
24 R. Bertani, P. Sgarbossa, A. Venzo, F. Lelj, M. Amati, G. Resnati, T. Pilati, P. Metrangolo and G. Terraneo, *Coord. Chem. Rev.,* 2010, **254**, 677-695 (DOI:10.1016/j.ccr.2009.09.035).
25 J. S. Ovens, A. R. Geisheimer, A. A. Bokov, Z. Ye and D. B. Leznoff, *Inorg. Chem.,* 2010, **49**, 9609-9616 (DOI:10.1021/ic101357y).
26 L. Koskinen, S. Jääskeläinen, P. Hirva and M. Haukka *Cryst. Growth Des.* 2015, **15**, 1160-1167 (DOI:10.1021/cg501482u)
27 F. R. Knight, K. S. Athukorala Arachchige, R. A. Randall, M. Buhl, A. M. Slawin and J. D. Woollins, *Dalton Trans.,* 2012, **41**, 3154-3165 (DOI:10.1039/c2dt12031c).
28 O. Hassel, H. Hope, N. A. Sörensen, H. Dam, B. Sjöberg and J. Toft, *Acta Chem. Scand.,* 1961, **15**, 407-416 (DOI:10.3891/acta.chem.scand.15-0407).
29 a) J. Lin, J. Martí-Rujas, P. Metrangolo, T. Pilati, S. Radice, G. Resnati and G. Terraneo *Cryst. Growth Des.* 2012, **12**, 5757−5762 (DOI: 10.1021/cg301262k), b) L. Meazza, J. Martí-Rujas, G. Terraneo, C. Castiglioni, A. Milani, T. Pilati, P. Metrangolo and G. Resnati *CrystEngComm*, 2011, **13**, 4427-4435 (DOI: 10.1039/c1ce05050h), c) J. Martí-Rujas, L. Meazza, G. K. Lim, G. Terraneo, T. Pilati, K. D. M. Harris, P. Metrangolo, and G. Resnati *Angew. Chem. Int. Ed.* 2013, **52**, 13444 –13448 (DOI: 10.1002/anie.201307552), d) I. D. Yushina, B. A. Kolesov, E. V. Bartashevich, *New J. Chem.* 2015, **39**, 6163-6170 (DOI:10.1039/c5nj00497), e) E. Bartashevich, E. Troitskaya, Á. M. Pendás, V. Tsirelson, *Comput. Theor. Chem.*, 2015, **1053**, 229-237 (DOI:10.1016/j.comptc.2014.09.024, f) E. V. Bartashevich, I. D. Yushina, A. I. Stash, V. G. Tsirelson, *Cryst. Growth. Des.*, 2014, **14**, 5674-5684 (DOI:10.1021/cg500958q g) E. V. Bartashevich, Y. V. Matveychuk, E.A. Troitskaya , V. G. Tsirelson, , *Comput. Theor. Chem.*, 2014, **1037**, 53-62 (DOI: 10.1016/j.comptc.2014.04.006), h) E. V. Bartashevich, V. G. Tsirelson, *Russ. Chem. Rev.*, 2014 **82**, 1181-1203 (DOI: 10.1070/RCR4440), i) E. V. Bartashevich, E. A. Troitskaya, V. G. Tsirelson, *Chem. Phys. Lett.*, 2014, **601**, 144-148 (DOI:10.1016/j.cplett.2014.04.004), j) E. V. Bartashevich, V. G. Tsirelson, *PCCP*, 2013, **15**, 2530-2538 (DOI: 10.1039/c2cp43416d).
30 M. Haukka, M. Ahlgrén and T. A. Pakkanen, *J. Chem. Soc. , Dalton Trans.,* 1996, , 1927-1933 (DOI:10.1039/dt9960001927).
31 M. Haukka, J. Kiviaho, M. Ahlgren and T. A. Pakkanen, *Organometallics,* 1995, **14**, 825-833 (DOI:10.1021/om00002a033).
32 Bruker AXS, APEX2 - Software Suite for Crystallographic Programs -, Bruker AXS, Inc., Madison, WI, USA, 2009, .
33 G. M. Sheldrick, *Acta Crystallogr. A.,* 2008, **64**, 112-122 (DOI:10.1107/S0108767307043930).
34 L. Palatinus and G. Chapuis, *J. Appl. Crystallogr.* 2007, **40**, 786-790 (DOI:10.1107/S0021889807029238).
35 L. J. Farrugia, *J. Appl. Crystallogr.* 1999, **32**, 837-838 (DOI:10.1107/S0021889899006020).
36 G. M. Sheldrick, SADABS - Bruker AXS scaling and absorption correction -, Bruker AXS, Inc., Madison, Wisconsin, USA, 2008.
37 E. F. Pettersen, T. D. Goddard, C. C. Huang, G. S. Couch, D. M. Greenblatt, E. C. Meng and T. E. Ferrin, *J. Comput. Chem.,* 2004, **25**, 1605-1612 (DOI:10.1002/jcc.20084 [doi]).
38 M. J. Frisch, G. W. Trucks, H. B. Schlegel, G. E. Scuseria, M. A. Robb, J. R. Cheeseman, G. Scalmani, V. Barone, B. Mennucci, G. A. Petersson, H. Nakatsuji, M. Caricato, X. Li, H. P. Hratchian, A. F. Izmaylov, J. Bloino, G. Zheng, J. L. Sonnenberg, M. Hada, M. Ehara, K. Toyota, R. Fukuda, J. Hasegawa, M. Ishida, T. Nakajima, Y. Honda, O. Kitao, H. Nakai, T. Vreven, M. A. Jr.J., J. E. Peralta, F. Ogliaro, M. Bearpark, J. J. Heyd, E. Brothers, K. N. Kudin, V. N. Staroverov, R. Kobayashi, J. Normand, K. Raghavachari, A. Rendell, J. C. Burant, S. S. Iyengar, J. Tomasi, M. Cossi, N. Rega, J. M. Millam, M. Klene, J. E. Knox, J. B. Cross, V. Bakken, C. Adamo, J. Jaramillo, R. Gomperts, R. E. Stratmann, O. Yazyev, A. J. Austin, R. Cammi, C. Pomelli, J. W. Ochterski, R. L. Martin, K. Morokuma, V. G. Zakrzewski, G. A. Voth, P. Salvador, J. J. Dannenberg, S. Dapprich, A. D. Daniels, Ö Farkas, J. B. Foresman, J. V. Ortiz, J. Cioslowski and D. J. Fox, *Gaussian 09, revision C.01*.,Gaussian, Inc., Wallinford CT, 2009.
39 J. P. Perdew, K. Burke and M. Ernzerhof, *Phys. Rev. Lett.,* 1997, **78**, 1396-1396 (DOI:10.1103/PhysRevLett.78.1396).
40 P. J. Hay and W. R. Wadt, *J. Chem. Phys.,* 1985, **82**, 299-310 (DOI:10.1063/1.448975).
41 A. W. Ehlers, M. Bohme, S. Dapprich, A. Gobbi, A. Hollwarth, V. Jonas, K. F. Kohler, R. Stegmann, A. Veldkamp and G. Frenking, *Chem. Phys. Lett.* 1993, **208**, 111-114 (DOI:10.1016/0009-2614(93)80086-5).
42 C. E. Check, T. O. Faust, J. M. Bailey, B. J. Wright, T. M. Gilbert and L. S. Sunderlin, *J. Phys. Chem. A,* 2001, **105**, 8111-8116 (DOI:10.1021/jp011945l).
43 N. Begovic, Z. Markovic, S. Anic and L. Kolar-Anic, *J. Phys. Chem. A,* 2004, **108**, 651-657 (DOI:10.1021/jp034492o).
44 R. F. W. Bader, *Atoms in Molecules - A Quantun Theory*, Clarendeon Press, Oxford, 1990.
45 T. A. Keith, *AIMAll 12.06.03*, TK Gristmill Software, Overland Park KS, USA, 2012..
46 U. Buontempo, A. Di Cicco, A. Filipponi, M. Nardone and P. Postorino, *J. Chem. Phys.,* 1997, **107**, 5720-5726 (DOI:10.1063/1.3396311).
47 Y. V. Nelyubina, M. Y. Antipin, D. S. Dunin, V. Y. Kotov and K. A. Lyssenko, *Chem. Commun.* 2010, **46**, 5325-5327 (DOI:10.1039/c0cc01094d [doi]).
48 L. Xu, J. Lv, P. Sang, J. Zou and Q. Yu, *J. Mol. Struct. THEOCHEM,* 2010, **953**, 170-174 (DOI:10.1016/j.theochem.2010.05.025).
49 C. Gatti, *Z. Kristallogr*. 2005, **220**, 399-457.
50 N. Cheng, Y. Liu, C. Zhang and C. Liu, *J. Mol. Model.* 2013, **19**, 3821-3829 (DOI:10.1007/s00894-013-1910-0).
51 M. T. Johnson, Z. Džolic, M. Cetina, O. F. Wendt, L. Öhrström and K. Rissanen, *Cryst. Growth Des.* 2012, **12**, 362-368 (DOI:10.1021/cg201170w).
52 E. Espinosa, I. Alkorta, J. Elguero, E. Molins, *J. Chem. Phys*. 2002, **117**, 5529-5542.
53 S. A. Sadjadi, C. F. Matta and I. P. Hamilton, *Can. J. Chem.* 2013, **91**, 583-590. (DOI: 10.1139/cjc-2012-0549)
54 M. Tuikka, M. Haukka *Acta Crystallogr. E, Cryst. Commun.* 2015, **71**, o463 (DOI: 10.1107/S2056989015010518).

For Table of Contents Use Only

SYNOPSIS TOC. The current paper introduces use of stable carbonyl containing ruthenium complexes, [Ru(bpy)(CO)2X2] (X=Cl, Br, I), as halogen bond acceptors for I2 halogen bond donor. Strong charge transfer to one I atom of the I_2 molecule weakens the halogen bond donor ability of the second iodine of I_2.